

Effect of Physical Parameters on Modelling for Reduction of Propylene in Converters

SANCHITA CHAUHAN

Department of Chemical Engineering and Technology

Panjab University, Chandigarh-160 014, India

Tel: (91)(172)2561355; E-mail: sanchita_pu@yahoo.co.in

Mathematical modelling for reduction in concentration of pollutant propylene in exhaust gas is carried out using catalytic converter. The performance of catalytic converters is highly dependent on its properties like cell density, catalytic surface area per unit reactor volume and length of the converter. The effect of varying these physical parameters on the conversion of propylene is analyzed.

Key Words: Catalytic converter, One-dimensional modelling, Cell density, Catalyst loading.

INTRODUCTION

At present monolithic converters are extensively used in pollution control applications, most notably as catalytic converters in automobile after-treatment of exhaust gases, where high flow rates and low pressure are the main requirements. In addition to pollution control applications there is also an increasing interest in the use of such reactors as combustion chambers¹.

Modelling plays an important part in development of catalytic converters. The original contributor for development of models for catalytic converter was Rutherford Aris². The experimental optimization based on engine bench and vehicle tests are extremely expensive and time-consuming as compared to modelling³. Numerical simulations help reduce the number of experiments and allow for interpreting in detail effect of some parameters otherwise neglected^{4,5}. There are many challenges that the developer of a mathematical model has to face. These challenges include lack of adequate kinetic data for different types of catalysts⁶.

The simplest and most common approach is a one channel model, which is assumed to be representative of the whole monolith. One-dimensional model predicts the monolith performance quite accurately for cold start conditions and requires about one-tenth computing time of the two-dimensional model⁷.

A one-dimensional model is proposed to bring about the reduction of hydrocarbon propylene taking into account both gaseous as well as catalytic reactions occurring in the converter. The performance of a converter depends upon the combined effect of heat transfer, mass transfer and chemical reactions. The mass and energy

balance equations for gas phase form a set of ordinary differential equations (ODEs) where as the energy balance equation for the solid catalyst temperature is partial differential equation (PDE). Results obtained show the effect of changing cell density, length of converter and catalyst loading on conversion of propylene.

The oxidation of propylene a fast oxidizing hydrocarbon⁸ is a highly exothermic reaction as is given by:



This reaction can take place in both homogenous and heterogeneous phases⁹ as shown in Table-1. Platinum suspended in alumina washcoat is used as catalyst for the catalytic reactions is shown in Fig. 1.

TABLE-1
RATE EXPRESSIONS FOR HOMOGENOUS AD CATALYTIC REACTIONS

Homogenous Reactions	Catalytic Reactions
$(-r)_{\text{homo}}(C_g, T_g) = k_{\text{homo}} \exp\left(-\frac{E_{\text{homo}}}{RT_g}\right) C_{\text{C}_3\text{H}_6} C_{\text{O}_2}$	$(-r)_{\text{cat}}(C_s, T_s) = k_{\text{cat}} \exp\left(-\frac{E_{\text{cat}}}{RT_s}\right) C_{\text{C}_3\text{H}_6}$
$k_{\text{homo}} 2.87 \times 10^{15} \text{ cm}^3 \text{ gmol}^{-1} \text{ s}^{-1}$	$k_{\text{cat}} 9.14 \times 10^4 \text{ cm s}^{-1}$
$E_{\text{homo}} 40,000 \text{ cal gmol}^{-1}$	$E_{\text{cat}} 12,000 \text{ cal gmol}^{-1}$

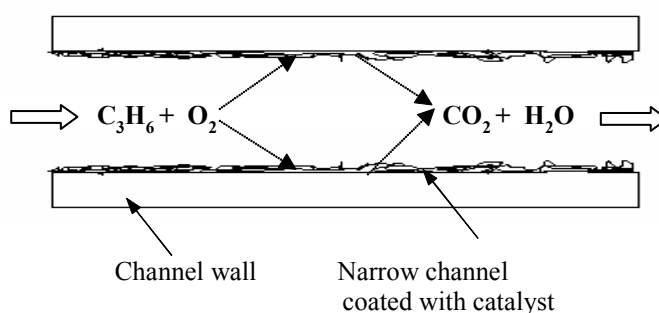


Fig. 1. Reaction in a monolith channel

ONE-DIMENSIONAL MODEL

In the one-dimensional model only axial gradients are considered for gas concentration, gas temperature and catalyst temperature.

Some assumptions made during modeling include:

- Negligible axial diffusion in gas phase.
- Monolith is cylindrical with circular cross-section channels. Non-uniform flow distribution inside the converter is neglected, as one single channel represents the entire monolith.

- Heat released by the catalytic reactions inside the washcoat was totally transported to the gas phase by convection.
- Heat transfer by radiation within channels and also heat exchange between the substrate and the surroundings at both inlet and outlet faces of the monolith was neglected.

At quasi steady state:

$$\frac{\partial C_g}{\partial t} = 0 \quad \text{and} \quad \frac{\partial T_g}{\partial t} = 0 \quad (1)$$

Mass balance in gas phase:

$$v(\partial C_g / \partial x) + (-r)_{\text{homo}}(C_g, T_g) + k_g S(C_g - C_s) = 0 \quad (2)$$

Mass balance in solid phase:

$$a(-r)_{\text{cat}}(C_s, T_s) = k_g S(C_g - C_s) \quad (3)$$

Energy balance in gas phase:

$$-C_{pg} v \rho_g (\partial T_g / \partial x) - h S(T_g - T_s) + (-\Delta H)(-r)_{\text{homo}}(C_g, T_g) = 0 \quad (4)$$

Energy balance in solid phase:

$$C_{ps} \rho_s (\partial T_s / \partial t) = \lambda_s (\partial^2 T_s / \partial x^2) + h S(T_g - T_s) + a(-\Delta H)(-r)_{\text{cat}}(C_s, T_s) \quad (5)$$

Initial conditions:

$$C_g(0, t) = C_g^0 \quad (\text{entering gas concentration all time}) \quad (6)$$

$$T_g(0, t) = T_g^0 \quad (\text{entering gas temperature all time}) \quad (7)$$

$$T_s(x, 0) = T_s^0 \quad (\text{solid catalyst temperature at the start}) \quad (8)$$

Boundary conditions:

$$\text{at } x = 0, (\partial T_s / \partial x) = 0 \quad (\text{lagging solid catalyst at entry}) \quad (9)$$

$$\text{at } x = L, (\partial T_s / \partial x) = 0 \quad (\text{lagging solid catalyst at exit}) \quad (10)$$

Eqns. 2 to 10 are made dimensionless using the following expressions:

$$C = C_g / C_g^0, \quad T_g' = T_g / T_g^0, \quad z = x / L, \quad T_s' = T_s / T_s^0, \quad t' = t / t_0 \quad (11)$$

Dimensionless equation for combined mass balance becomes:

$$\left(\frac{dC'}{dz} \right) = -\chi C' e^{(-E_{\text{cat}} / RT_s')} - \omega C'^2 e^{(-E_{\text{homo}} / RT_g')} - \theta C' e^{(-E_{\text{homo}} / RT_g')} \quad (12)$$

Dimensionless equation for energy balance for gas phase:

$$\left(\frac{dT_g'}{dz} \right) = \phi (T_s' - T_g') + \sigma C' e^{(-E_{\text{homo}} / RT_g')} + \psi C'^2 e^{(-E_{\text{homo}} / RT_g')} \quad (13)$$

Dimensionless equation for energy balance for solid phase:

$$\left(\frac{dT_s'^2}{dz^2}\right) = -\gamma C' e^{(-E_{cat}/RT_s')} + \alpha (T_s' - T_g') + \delta \left(\frac{dT_s'}{dt'}\right) \quad (14)$$

where, χ , w , θ , ϕ , σ , ψ , γ , α , and δ are dimensionless numbers as shown in Table-2.

TABLE-2
DIMENSIONLESS NUMBERS

$\omega = (C_g^0) \frac{L \left(\frac{b}{a}\right) k_{homo}}{v}$	$\gamma = (C_g^0) \frac{aL^2(-\Delta H)k_{cat}}{\lambda_s T_g^0}$
$\theta = (C_g^0) \frac{L \left(M - \frac{b}{a}\right) k_{homo}}{v}$	$\phi = \frac{4Lh}{v\rho_g C_{pg} d}$
$\sigma = (C_g^0)^2 \frac{L(-\Delta H) \left(M - \frac{b}{a}\right) k_{homo}}{T_g^0 C_{pg} v\rho_g}$	$\chi = \frac{Lak_{cat}}{v}$
$\psi = (C_g^0)^2 \frac{L(-\Delta H) \left(\frac{b}{a}\right) k_{homo}}{T_g^0 C_{pg} v\rho_g}$	$\alpha = \frac{4hL^2}{\lambda_s d}$
	$\delta = \frac{\rho_s C_{ps} L^2}{\lambda_s t_0}$

Dimensionless initial conditions:

$$C'(0, t') = 1.00, \quad T_g'(0, t') = \frac{T_g}{T_g^0}, \quad T_s'(z, 0) = \frac{T_s}{T_s^0} \quad (15)$$

Dimensionless boundary conditions:

$$\text{at } z = 0.0, \quad \frac{dT_s'}{dz} = 0 \quad (16)$$

$$\text{at } z = 1.0, \quad \frac{dT_s'}{dz} = 0 \quad (17)$$

Eqns. 12 and 13 are ODEs and eqn. 14 is a PDE.

Numerical scheme: Eqns. 12-14 are all coupled; hence they are solved at the same time. The time derivative term does not exist in the ODEs but is present in the PDE. The ODEs are solved using Runge-Kutta method of fourth order and the PDE by backward implicit scheme. Effect of grid sizes has been studied.

RESULTS AND DISCUSSION

Results are derived for variation of propylene concentration with time for different cell density, catalyst loading and length of the converter. Exhaust gas propylene (1900 ppm) at 390 °C undergoes oxidation reaction in the converter (initially at 45 °C). The computations are stopped when propylene concentration decrease beyond 0.2000.

Fig. 2 shows the variation of exit concentration of propylene with time by varying the cell density. At dimensionless time 6.00 the concentrations of propylene are 0.9832, 0.9179, 0.8576 and 0.7293 for cell densities 16, 62, 93 and 155 cells/cm². At dimensionless time 7.50 the concentrations of propylene are 0.9631, 0.7872, 0.5942 and 0.2036, respectively for cell densities 16, 62, 93 and 155 cells/cm². Increasing the cell density of the converter increases its surface area available for the catalytic reactions. More the surface area available faster would be the reaction and hence more would be the conversion.

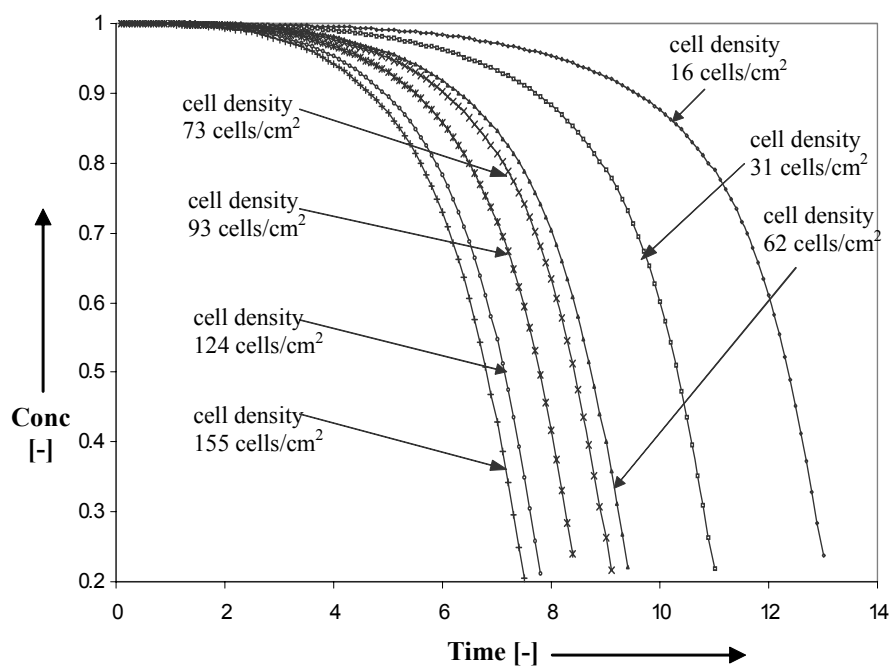


Fig. 2. Exit propylene gas concentration variation with time for different values of cell density

Fig. 3 shows the effect of varying the catalyst loading 'a' in the converter on the exit concentration of propylene gas in the converter. For this study standard loading 'a' is taken as 268 cm² Pt/cm³ reactor. At dimensionless time 4.00 the concentrations are 0.9730, 0.9870, 0.9936 and 0.9968 for catalyst loading represented by 8a,

4a, 2a and a, respectively showing almost similar values of concentration of propylene. However with increase of time appreciable difference is observed in the values of propylene concentrations, the fastest conversion of propylene occurring at highest value of catalyst loading. At time 8.00 the propylene concentrations are 0.3759, 0.8296, 0.9346 and 0.9706 and at time 8.30 the concentrations are 0.2086, 0.7953, 0.9250 and 0.9672, respectively for catalyst loading represented by 8a, 4a, 2a and a. Results indicate more conversion occurs as time increases and the conversion is faster in case of higher catalyst loading due to increased rate of catalytic reactions.

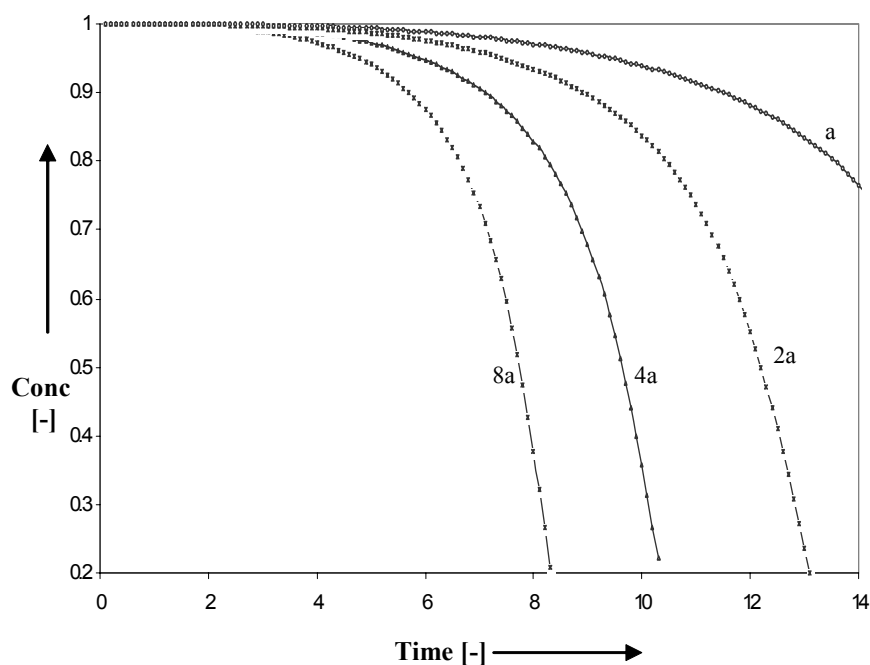


Fig. 3. Exit propylene gas concentration variation with time for different values of catalyst loading

Fig. 4 shows the effect of length of the converter on conversion of propylene. At dimensionless axial length of 0.3, 0.5, 0.7 and 1.00 the concentration of propylene are 0.8719, 0.8038, 0.7479 and 0.6786 at time 9.0, respectively. At dimensionless axial length of 0.3, 0.5, 0.7 and 1.00 the concentration of propylene are 0.4989, 0.3661, 0.2915 and 0.2221 for dimensionless time 10.3, respectively. Shorter lengths result in lesser conversion. So the results indicate that increasing the length increases the residence time in the converter and hence more conversion of propylene takes place.

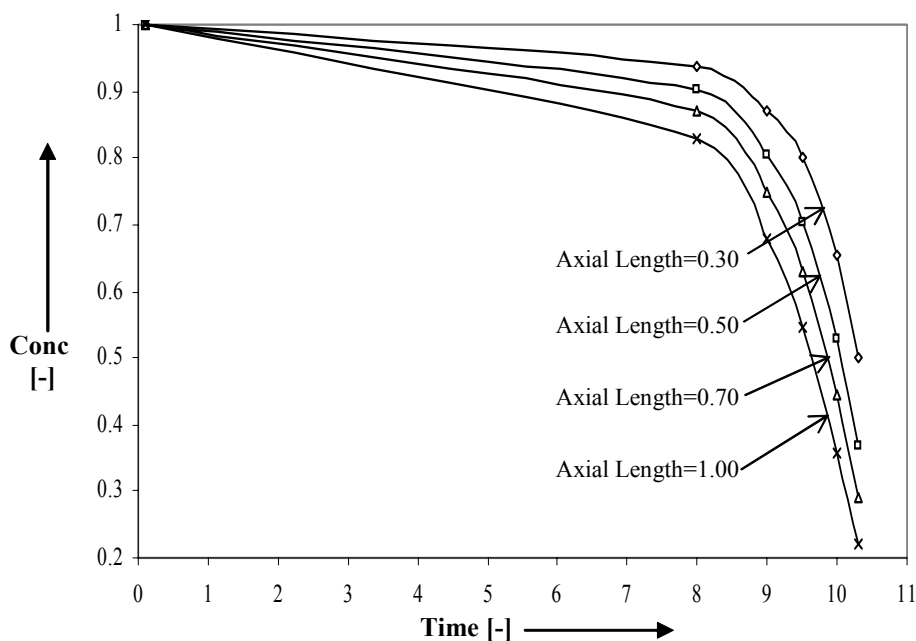


Fig. 4. Effect of converter length on propylene gas concentration with time

Nomenclature

a	Catalytic surface area per unit reactor volume ($\text{cm}^2 \text{cm}^{-3}$)
b/a	ratio of stoichiometric coefficients for oxygen and propylene.
C	Concentration of the propylene (gmol cm^{-3})
C_p	Specific heat ($\text{cal g}^{-1} \text{K}^{-1}$)
d	Hydraulic diameter (cm)
E_{cat}	Activation energy for the catalytic reaction (cal gmol^{-1})
E_{homo}	Activation energy for the homogenous reaction (cal gmol^{-1})
h	Heat transfer coefficient ($\text{cal cm}^{-2} \text{s}^{-1} \text{K}^{-1}$)
$-\Delta H$	Heat of reaction (cal gmol^{-1})
k_g	Mass transfer coefficient (cm s^{-1})
k_{cat}	Rate constant for catalytic reaction (cm s^{-1})
k_{homo}	Rate constant for homogenous reaction ($\text{cm}^3 \text{gmol}^{-1} \text{s}^{-1}$)
L	Length of monolith (cm)
M	Ratio of incoming oxygen and propylene.
R	Gas constant ($\text{cal gmol}^{-1} \text{K}^{-1}$)
S	Geometric surface area per unit reactor volume ($\text{cm}^2 \text{cm}^{-3}$)
T	Temperature (K)
t	Time (s)
v	Gas velocity (cm s^{-1})
x	Axial coordinates (cm)

z	Dimensionless axial coordinates
λ	Thermal conductivity ($\text{cal cm}^{-1} \text{s}^{-1} \text{K}^{-1}$)
ρ	Density (g cm^{-3})

Superscript:

o	Initial conditions
'	Dimensionless quantities

Subscript:

s	Solid
g	Gas

ACKNOWLEDGEMENT

The support of Prof. V. K. Srivastava (Director, ABES Institute of Technology, Ghaziabad, India) for his invaluable inputs and advice during this work is gratefully acknowledged.

REFERENCES

1. R.E. Hayes, S.T. Kolaczowski and W.J. Thomas, *Comput. Chem. Eng.*, **16**, 643 (1992).
2. K. Zygourakis, *Chem. Eng. Sci.*, **44**, 2075 (1989).
3. D.K.S. Chen, S.H. Oh, E.J. Bissett and D.I.V. Ostrom, SAE Paper 880282, 3, 177 (1988).
4. S.H. Oh and J.C. Cavendish, *Ind. Eng. Chem. Prod. Res. Dev.*, **22**, 509 (1983).
5. C.J. Pereira, J.E. Kubsh and L.L. Hegedus, *Chem. Eng. Sci.*, **43**, 2087 (1988).
6. T. Shamim, H. Shen, S. Sengupta, S. Son and A.A. Adamczyk, *J. Engg. For Gas Turbines and Power*, **124**, 421 (2002).
7. R.H. Heck, J. Wei and J.R. Katzer, *AIChE J.*, **22**, 477 (1976).
8. D. Cundari and M. Nutti, SAE Paper 910668, 4, 258 (1991)
9. T. Ahn, W.V. Pinczewski and D.L. Trimm, *Chem. Eng. Sci.*, **41**, 55 (1986).

(Received: 8 January 2008;

Accepted: 25 September 2008)

AJC-6891